J. RADIAT. RES., 40, 145–158 (1999)

Single- and Double-Strand Breaks in Solid pBR322 DNA Induced by Ultrasoft X-rays at Photon Energies of 388, 435 and 573 eV

AKINARI YOKOYA[1]*, RITSUKO WATANABE[2] and TAKEHIRO HARA[3]

[1]Department of Synchrotron Radiation Research, Japan Atomic Energy Research Institute, Hyogo 678–1201, Japan
[2]Department of Environmental Safety, Japan Atomic Energy Research Institute, Tokai-mura 319–1195, Japan
[3]College of Science, Rikkyo University, Tokyo 171–8501, Japan
(*Received, January 25, 1999*)
(*Revision received, April 6, 1999*)
(*Accepted, April 19, 1999*)

Monochromatic ultrasoft X-rays/DNA strand break/Synchrotron radiation/Nitrogen K-edge/Oxygen K-edge

We measured strand breaks of pBR322 plasmid DNA irradiated with ultrasoft X-rays using monochromatic synchrotron radiation as a light source. Three photon energies, 388, 435 and 573 eV, a value below and above the nitrogen K-edge and above the oxygen K-edge, respectively, were chosen for the irradiation experiments as they have an equivalent photon transmittance of the sample. Irradiated DNA was analyzed by agarose gel electrophoresis and the numbers of single-and double-strand breaks (ssb and dsb) were determined by measuring the band intensity on the gel after ethidium bromide staining. The action cross-sections for the ssb and dsb slightly increased with the photon energy. The ratio between 388 and 573 eV was about 1.5 for both forms of strand breaks. The absorbed energy required for a strand break was about 60 eV for ssb and 1 keV for dsb, less than one fifth of the values obtained previously in the 2 keV region. On the other hand, the absorbed energies per strand break, as well as the ratio of the action cross-section for the ssb to that for the dsb, were constant regardless of the photon energy used. The K-shell photoabsorption on carbon, nitrogen and oxygen atoms in the DNA molecule, followed by an Auger cascade, induced DNA strand breaks with a constant efficiency in terms of the absorbed energy. These results indicate that the strand breaks of the DNA molecule in the solid state are mainly caused by the photo- and Auger-electrons and the efficiency of the strand breaks little depends on the atoms ejecting these secondary electrons.

INTRODUCTION

Monochromatic ultrasoft X-rays below 1 keV are an attractive light source for selecting an

*Corresponding author: Phone; +81–7915–8–0884, Fax; +81–7915–8–2740, E-mail; yokoya@spring8.or.jp

exclusive K-shell photoabsorption on carbon (284 eV), nitrogen (410 eV) or oxygen (543 eV) in biological materials, followed by the ejection of low energy secondary electrons from the target atom. Theoretical analysis has predicted that such low-energy electron tracks produce dense ionization and thus cause local multiple damage to DNA molecules, which is critical to the radiobiological consequences[1–3]. On the other hand, studies of the DNA lesions induced by ultrasoft X-rays have suffered from the lack of a monochromatic photon source intense enough to induce detectable amounts of molecular damage in this energy region.

An advanced X-ray irradiation technique utilizing synchrotron radiation as the photon source has advanced studies into the radiobiological effects of monochromatic soft X-rays[4–6]: the K-shell photoabsorption effects of phosphorus atoms on the molecular dissociation of DNA or relative compounds have been investigated using 2.1 keV photons[7–10]. In the energy region below 1 keV excluding the UV region, however, little is known as to the irradiation effects on the DNA molecule. X-ray Absorption Near-Edge Structure (XANES) spectra of DNA were measured around the carbon and nitrogen K-edge using a high resolution monochromator combined with synchrotron-radiation-beamlines[11,12]. It would be interesting to elucidate how the absorption structure affects the induction of DNA damage.

In this report, the photoabsorption spectrum of DNA was measured in the ultrasoft X-ray region using thin DNA film as a basis for radiobiological studies. Based on obtained absolute absorption cross-sections around the nitrogen and oxygen K-edge, three photon energies penetrating the sample for the same depth were selected as the irradiation energies. The action cross-sections of the single- and double strand breaks (ssb and dsb) of pBR322 plasmid DNA in the solid state were determined and converted to energies required per ssb and dsb using the absorption cross sections.

MATERIALS AND METHODS

Preparation of thin DNA films for measurement of the absorption spectrum

Calf thymus DNA (Na salt, type 1) (Sigma Co., St. Louis, USA) was dissolved in distilled water at three different concentrations, 1.24 , 0.62 and 0.33 mg/ml. The DNA solutions (100 μl) were dried on a Ni mesh support (28 ∞ 28 μm^2 pore size; 17 μm space; 10 μm thickness; Dainippon Screen Co., Kyoto, Japan). Dry DNA films of each thickness were prepared as circular samples of 9 mm diameter. The sample was supported by a sample holder made of acrylic resin.

The surface of the films was observed with a Nomarski interference microscope (MRC-600, Bio-Rad, California, USA). No pinhole or breakage was observed for the two thicker samples. However, several pin-holes were observed for the thinnest sample, and thus for absorption measurements, an area without pinholes was selected using a stainless steel orifice (2 ∞ 2 mm) glued to the sample holder.

To estimate the surface density of the film, the UV absorbance of the DNA films was measured with a UV spectrometer (DU-65 spectrometer, Beckman, California, USA) in ambient air (about 50% relative humidity) with reference to a Ni mesh without DNA. The light scattering component of the samples below 300 nm was estimated by extrapolating the absorption spectrum

between 710 nm and 340 nm, and subtracted from the measured absorbance in order to obtain the net absorbance. The net absorbance at 260 nm was converted to the surface density of DNA using the factor, 0.27 g/m^2 (= 0.50/1.88) per unit absorbance at 260 nm, based on the following assumption: the absorbance of the dry DNA at about 50% relative humidity is 1.88 times higher than that of the wet DNA[13], and wet DNA of 0.50 g/m^2 gives one unit of absorbance at 260 nm[14]. Furthermore, dry DNA at 0% relative humidity or in a vacuum inevitably contains bound water molecules; we adopted the value of 2.5 bound water molecules per nucleotide[15], so the DNA film in vacuum consists of 0.88 parts DNA and 0.12 parts water. The calculated surface densities of the DNA films thus obtained are listed in Table 1.

Table 1. Surface density of the DNA films measured with UV-absorbance.

Sample	Absorbance at 260 nm	Surface density[a] (g/m^2)
1	0.46	0.139
2	1.21	0.365
3	2.82	0.852

[a]The values include the bound water (2.5 molecules per nucleotide).

Ultrasoft X-ray absorption spectrum of DNA film

Ultrasoft X-ray absorption was measured at the beamline 12A equipped with a 2m-spherical grating monochromator in the Photon Factory (PF), Institute for Materials Structure Science. The energy resolution, E/ΔE, was about 300 and 1000 with a slit width of 100 and 20 μm, respectively. The photon energy was calibrated with the resonance peak of the 1s state to the π^* antibonding state of nitrogen (400.96 eV) and oxygen molecule (530.8 eV)[16] by measuring the photoabsorption spectrum of air.

A schematic layout of the measurement system is shown in Fig. 1. The DNA films were set in the vacuum chamber for biological irradiation experiments[6]. The beam was adjusted to a 2 ∞ 2 mm^2 area with a cross-screen steel slit set at the upper stream of an Au mesh monitor. The intensity of the beam was measured by an Au plate downstream of the sample as a photoelectron current, and monitored by an Au mesh set upstream of the sample. Transmittance (T) was given by the ratio of Au-plate output over Au-mesh output between the DNA sample and the reference sample (Ni-mesh support without DNA); absorbance is $-\log_{10}T$.

The uniformity of the sample thickness was surveyed as follows: the transmittance was measured by scanning the sample at 200 μm steps in both the vertical and horizontal direction using a narrow beam of 200 μm diameter at 900 eV, at which high transmittances (about 50% for the thickest sample) ensured enough intensity. The relative errors of the absorbance of the samples are indicated by error bars in Fig. 4.

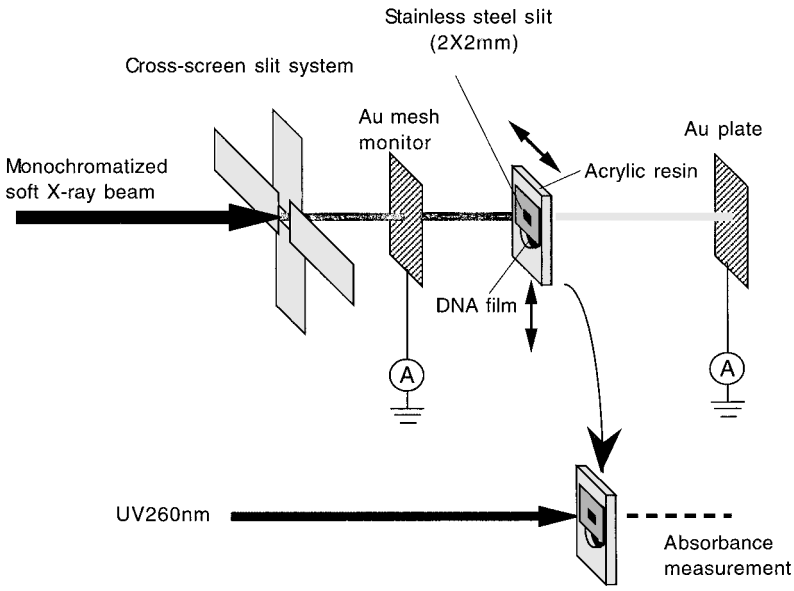

Fig. 1. Schematic layout for ultrasoft X-ray photoabsorption spectrum measurement.

Plasmid DNA sample for irradiation experiments

pBR322 plasmid DNA solution (1 μg/μl in a buffer of 10 mM tris and 1mM EDTA (pH 8.0); Takara, Japan) was diluted with the same volume of distilled, double-deionized water. One μl of the solution was dried in air on a hydrophilic area (2×2 mm^2) of a glass plate, of which the peripheral area was made hydrophobic with a spray (Polyfron Spray Wax, Osaka, Japan). The dry DNA film contained 0.5 μg DNA and 0.9 μg of the buffer solute in an area of 2×2 mm^2 with 0.35 g/m^2 thickness, and differed from the samples in our previous study (1 μg DNA and 0.54 μg of the buffer solute[10]) in which the pBR322 DNA purified from *Escherichia coli* cells harboring the plasmid was used. The mass fraction in the produced pBR322 DNA sample was 0.341 for DNA, 0.046 for bound water and 0.613 for the buffer solute.

Monochromatic ultrasoft X-ray irradiation

The plasmid DNA samples were irradiated with monochromatic ultrasoft X-rays at the three photon energies of 388, 435 and 573 eV, corresponding to a value below and above the nitrogen K-edge (410 eV) and above the oxygen K-edge (543 eV), respectively. We chose these three photon energies as they penetrated to the same depth in the sample (see RESULTS). The total mass photoabsorption coefficients of the sample were calculated as the weighted averages of DNA cross-sections obtained in this paper and of the buffer solutes calculated from values the tabulated by Henke et al[17].

The photon flux of the beam was measured using a photodiode (AXUV-100, International Radiation Detectors Inc., California, USA) in stead of the ionization chamber we used in our previous work[10] because the strong attenuation of the ultrasoft X-rays prevented us from extract-

ing the beam into the air . The output current of 1 nA from the photodiode at the photon energy of 500 eV is calculated to be equivalent to 4.54×10^7 photons·sec^{-1}, assuming the quantum efficiency of the diode to be 3.63 eV/electron as recommended by the maker.

The correction factors for the decrease in the ultrasoft X-ray intensity in the sample were calculated using

$$(1 - \exp(-\sigma\,(\mu/\rho)_{\text{sample}}))/\,\sigma\,(\mu/\rho)_{\text{sample}}, \tag{1}$$

where σ is the surface density (0.35 g/m^2; see above) of the sample, and the factors are shown in the fifth column of Table 3.

Estimation of the absorbed dose

The absorbed dose (Gy) is given by the following equation from the photon fluence (m^{-2}) after the correction by the correction factor (equation 1):

$$\text{Absorbed dose} = \text{photon fluence} \propto [E \times 1.6 \propto 10^{-19}\,(\mu/\rho)_{\text{sample}} \times 10^3], \tag{2}$$

where E is the photon energy in eV, 1.6×10^{-19} J per eV, $(\mu/\rho)_{\text{sample}}$ the mass absorption cross section in m^2/g, and 10^3 g per kg. The $(\mu/\rho)_{\text{sample}}$ and the calculated conversion factor are listed in Table 3.

Measurement of single- and double-strand breaks

The DNA sample was redissolved in 25 μl of Tris-EDTA buffer (10 mM tris and 1mM EDTA (pH 8.0); Takara, Japan), supplemented with a 1/10 volume of loading buffer (40% sucrose and 0.25% bromophenol blue) and placed in a slot of the 1.7% agarose gel. Electrophoresis was carried out at 4.2 V/cm for 3 hours at 4°C in a TAE buffer (40 mM Tris, 5 mM sodium acetate and 1 mM EDTA, adjusted to pH 7.8 with acetic acid). After staining with ethidium bromide, fluorescence images were taken with a CCD camera, and the DNA amount was determined by measuring the fluorescence intensity. The numbers of single and double strand breaks were calculated using the equation described by Povirk et al[18].

RESULTS

Ultrasoft X-ray photoabsorption spectra of the DNA film

Figure 2 shows the photoabsorption spectra of the DNA film at a resolution of 300 (the entrance and exit slit were 100 μm). Large resonance peaks were observed at 407 and 540 eV around the nitrogen and oxygen K-edge structure. At a higher resolution (1000 with 20 μm slits), the peak on the oxygen K-edge split into two, a large peak at 541 eV and a small one at 532 eV (Fig. 3).

The absorbance of the DNA at several photon energies plotted against the sample surface density showed a linear relationship (Fig. 4), indicating Lambert's law ($-\log_{10}(T) = \mu d$, where T

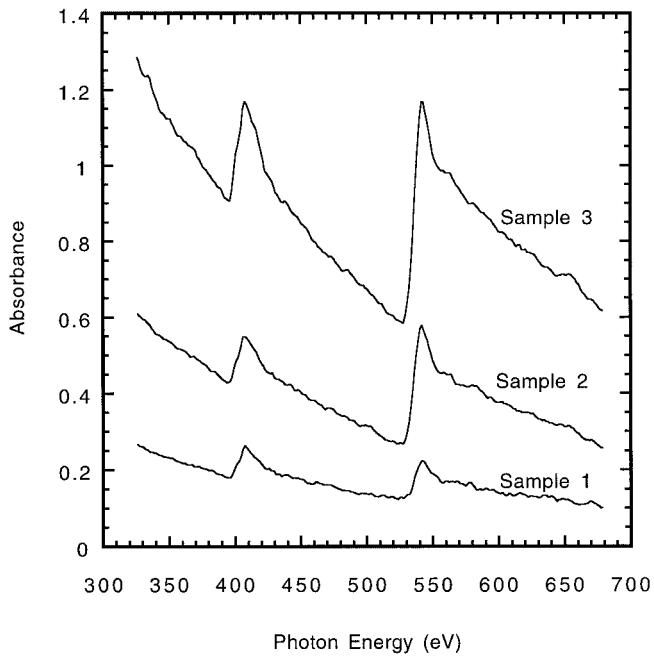

Fig. 2. Ultrasoft X-ray absorption spectra of thin DNA films with three different thicknesses around the nitrogen and oxygen K-edge (slits 100 μm). The sample numbers correspond to those in Table 1.

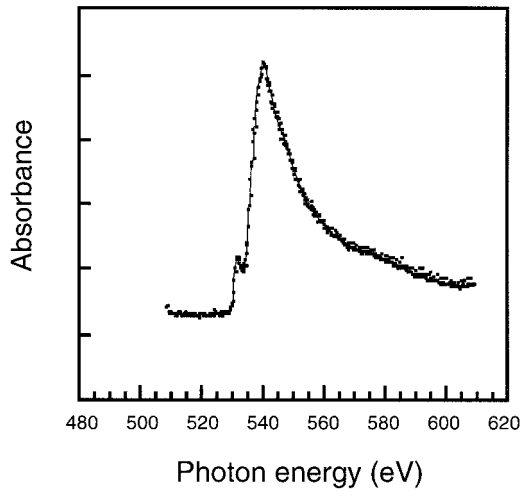

Fig. 3. Fine structure of the absorption spectrum of the DNA film (sample 2) around the oxygen K-edge with higher energy resolution (slits 20 μm).

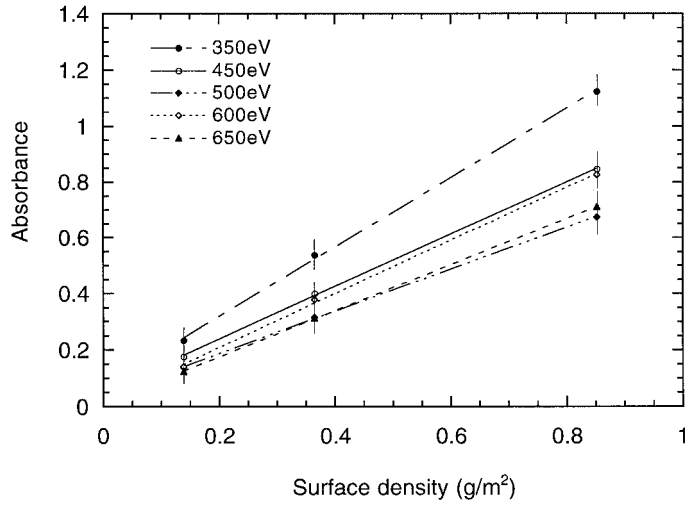

Fig. 4. Linear relationship between the absorbance shown in Fig. 2 and the surface densities of the three DNA films at 350, 450, 500, 600 and 650 eV. The lines were drawn by the least squares method. The bars on the points indicate the relative errors (see MATERIALS AND METHODS).

is transmittance, μ is absorption coefficient and d is thickness of the material) is applicable to our data. Thus, the slopes of the lines indicate the mass photoabsorption cross-sections, μ/ρ (m^2/g) of the DNA film at each energy, which are listed in Table 2. The absorption cross-sections of the DNA molecule without the bound water were obtained as {(absorption cross-section of sample) – (absorption cross-section of water) × (mass fraction of water)} / (mass fraction of DNA), which is easily derived from the definition, (absorption cross-section) = (absorbance) / (surface density). The absorption cross-sections of water were calculated using tabulated values[17], and the mass fractions of water and DNA were 0.12 and 0.88 (see MATERIALS AND METHODS).

The mass photoabsorption cross-section of DNA can be calculated by summing the cross-sections of each element, $(\mu/\rho)_i$, and multiplying by the weight fraction of the atoms as follows:

$$\Sigma\,(\mu/\rho)_i \cdot n_i \cdot M_i \,/\, \Sigma\, n_i \cdot M_i,$$

where n_i is the number of i element in a DNA molecule, and M_i is the atomic weight of the element. The values at measured photon energies were obtained by the interpolation of tabulated values[17]. Using (adenine + thymine) : (guanine + cytosine) = 1 : 1.35 in the calf thymus DNA molecule[19], the abundance of atoms per nucleotide pair in the DNA sodium salt was obtained, H; 22.57, C; 19.57, N; 7.42, O; 13.42, P; 2.00 and Na; 2.00. The calculated values were in good agreement with the experimental ones at the off-resonance peak energy (Table 2).

Photoabsorption cross-sections of the pBR322 DNA sample which consisted of one part DNA (including bound water) and 1.8 parts buffer solutes were calculated at the irradiation energies as weighted averages of the cross-sections of both components. The cross-sections of the

Table 2. Mass photoabsorption cross-sections (μ/ρ) of the DNA film containing 2.5 bound water molecules per nucleotide, and those calculated using the tabulated values of Henke et al[17].

Photon energy (eV)	Mass photoabsorption cross-section (μ/ρ) (m^2/g)		Ratio (measured/calculated)
	Measured[a]	Calculated	
350	1.24 (1.41)[b] ± 0.13	1.48	0.84
388[c]	1.05 (1.19) ± 0.11	1.13	0.93
435[c]	1.01 (1.14) ± 0.11	1.24	0.81
450	0.94 (1.06) ± 0.10	1.09	0.86
500	0.75 (0.86) ± 0.08	0.86	0.87
573[c]	1.06 (1.20) ± 0.10	1.25	0.85
600	0.96 (1.09) ± 0.09	1.11	0.87
650	0.83 (0.94) ± 0.08	0.91	0.91

[a] (value measured for the sample area of 2∞ 2 mm^2) ± (variation within the area estimated using a narrow beam of 200 μm), for details see MATERIALS AND METHODS.

[b] values for DNA without bound water (see RESULTS).

[c] These photon energies were used for irradiation of pBR322 plasmid DNA.

Table 3. Mass photoabsorption cross-section (μ/ρ), correction factor for the decrease in the X-ray intensity in the sample and conversion factor from photon fluence (m^{-2}) to absorbed dose (Gy) for DNA sample.

Photon energy (eV)	(μ/ρ) (m^2/g)			Correction factor[d]	Conversion factor (∞ 10^{-14})[e]
	DNA[a]	Buffer solute[b]	DNA sample with buffer[c]		
388	1.05	1.29	1.20	0.817	7.46
435	1.01	1.26	1.16	0.822	8.08
573	1.06	1.24	1.17	0.821	10.74

[a] Cited from Table 2 for DNA with 2.5 bound water molecules per nucleotide.

[b] The values were calculated by summing the cross-sections of each constituent element, which were obtained by interpolation of values tabulated by Henke et al[17] multiplied by the weight fraction of the element[10].

[c] $(\mu/\rho)_{sample} = 0.387 \times (\mu/\rho)_{DNA} + 0.613 \infty (\mu/\rho)_{buffer}$, because the mass fraction of the sample was 0.387 for DNA including the bound water and 0.613 for the buffer solute (see MATERIALS AND METHODS).

[d] See equation 1 in MATERIALS AND METHODS.

[e] The factor for converting from photon fluence (m^{-2}) to absorbed dose (Gy) calculated by equation 2 in MATERIALS AND METHODS.

pBR322 DNA were assumed to be the same as those experimentally measured for calf thymus DNA (see Table 2). The cross-sections of the buffer solutes were calculated based on the composition of atom, H; 13.2, C; 5.0, N; 1.2, O; 3.8, Na; 0.3, Cl; 0.56[10]. The estimated total cross-sections (Table 3) agree within 3% at the three photon energies. Based on the spectrum thus

obtained, we chose three photon energy, 388, 435 and 573 eV, for selectively irradiating the K-shell of carbon, nitrogen and oxygen, respectively, without changing the penetration depth in the sample.

Induction of strand breaks

The number of ssb (n_{ssb}) or dsb (n_{dsb}) linearly increased with the fluence as plotted in Fig. 5 for all ultrasoft X-ray energies. The slopes of the lines represent the action cross-sections of the

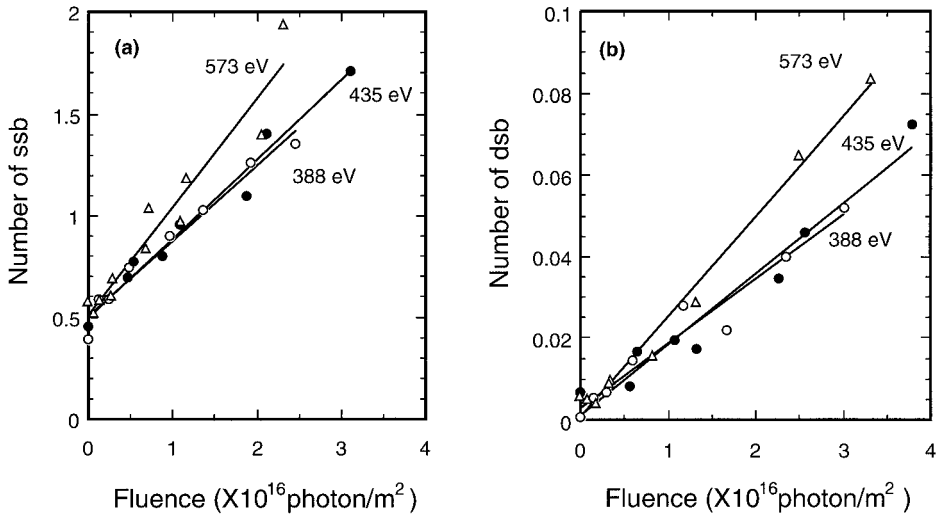

Fig. 5. Induction of ssb (a) and dsb (b) in the plasmid at three photon energies. The lines were fitted by the least-squares method.

Table 4. Cross-section of pBR322 plasmid DNA for strand-break induction, number of photoabsorption per strand break and energy required for a strand break.

Photon energy (eV)	Cross-section ($\propto 10^{-18}m^2$)			Number of photo-absorption per strand break[c]		absorbed energy required for a strand break (eV/sb)[d]	
	Action[a]		Absorption of DNA[b]				
	ssb	dsb		ssb	dsb	ssb	dsb
388	37	2.0	6.1	0.16	3.1	60	1140
435	39	2.1	5.8	0.15	2.8	62	1150
573	52	3.0	6.1	0.12	2.0	62	1070

[a] The cross-sections were reciprocals of the photon fluence giving one strand break.

[b] Absorption cross-sections (m^2/g) of DNA without bound water (Table 2) were converted to m^2/molecule by multiplying by the molecular weight of the pBR322 molecule (4.79×10^{-18} g).

[c] (Absorption cross-section)/(action cross-section).

[d] See RESULTS.

DNA strand breaks per fluence (Table 4). The cross-sections for both of the strand breaks slightly increased with the photon energy; the ratio between 388 and 573 eV was 1.4 for ssb and 1.5 for dsb. On the other hand, the absorption cross-sections of DNA were relatively constant over this energy range, indicating that the ratio of the absorption cross-section to the action cross-section, in other words the number of photons absorbed per strand break per molecule, decreased with increasing photon energy. The ratios between the ssb and the dsb did not seem to depend on the photon energy (ranging from 17 to 18) in this energy region.

The photon fluence required to induced one strand break was the reciprocal of the action cross-section and converted to the absorbed dose (Gy) using the factor in Table 3. These absorbed doses multiplied by the weight of the pBR322 DNA (4.79×10^{-18} g) and by 6.24×10^{18} eV per J were the absorbed energies in eV per strand break (the last two columns of Table 4). These energies were constant regardless of the photon energy, and this constancy will be discussed in the Discussion.

DISCUSSION

Photoabsorption cross-section of DNA in the ultrasoft X-ray region

The mass photoabsorption cross-section of DNA was experimentally determined for the first time around the nitrogen and oxygen K-edge in the ultrasoft X-ray region using Lambert's law. For an exact estimation of the number of photons absorbed by the sample for the irradiation experiments, the values obtained here would be more accurate than the calculated ones which are not valid at or near the resonance peaks. It is noteworthy that the values measured at the off-resonance peaks matched well those calculated using the tabulated values[17]. Though the difference between the two kinds of values was within the range of experimental error (Table 2), a closer look reveals that the experimental values were slightly smaller than the calculated ones. This may be explained by the uncertainty as to the number of bound water molecules in DNA: we assumed a value of 2.5 bound water molecules per nucleotide[15] in the calculation.

Initial photoabsorption sites and strand break induction

In the energy region of this experiment, the photons are predominantly absorbed by K-shell electrons of the carbon, nitrogen and oxygen atoms in DNA. We examined how these K-shell photoabsorptions affect the induction of the DNA strand breaks at three photon energies with the same photoabsorption cross-section, which enabled us to directly compare the efficiency of the strand breaks between these energies without the need to consider photon-beam attenuation in the sample. The results (Table 4) clearly showed that the energies required for a strand break were constant at 388, 435 and 573 eV.

To show quantitatively the difference in photoabsorption sites at the three photon energies, fractions of the K-shell and other shells of photoabsorption cross-sections of each atom in the DNA sample were calculated as follows: the logarithm of the mass photoabsorption coefficients[17] was plotted against the $-\log_{10}$ (photon energy), and the ratio of the two parts of the coefficients, one of which is originated from the K-shell photoabsorption and one from other shells, was

Table 5. Fractional contribution of the photoabsorption cross-sections of each atom constituting the pBR322 DNA sample.

Photon	Carbon		Nitrogen		Oxygen		Other atoms
(eV)	K-shell	Others	K-shell	Others	K-shell	Others	
388	0.663	0.022	–	0.013	–	0.067	0.235
435	0.507	0.017	0.230	0.007	–	0.050	0.189
573	0.264	0.009	0.130	0.004	0.466	0.025	0.102

estimated from the linear interpolation on the graph. Thus, the photoabsorption cross-sections of the K-shell and other shells were obtained using the ratios and the weighted atomic composition of the sample (Table 5). The largest photoabsorption site is the K-shell of carbon at 388 and 435 eV and of oxygen at 543 eV. In spite of the difference in major photoabsorption sites, the energy required for a strand break did not depend on the photon energy (Table 4), indicating that the efficiencies of the strand break induction on the basis of absorbed dose were constant regardless of the K-photoabsorption sites. Concerning the phosphorus K-absorption (around 2153 eV), similar conclusions had been obtained for the strand break induction of pBR322 plasmid DNA[10], dissociation of pentadeoxythymidylic acid[8] and 2'-deoxyadenylyl-(3'-5')-2'-deoxyadenosine[7]. These results showed that a marked change of the strand-break efficiency would not be caused by soft X-rays within the narrow energy range around the K-edges in a solid DNA molecule.

The absorbed energies in eV per strand break listed in the last two columns of Table 4 were about 60 eV for ssb and 1 keV for dsb. These values were considerably smaller than those obtained in our previous work using 2.1 keV photon (about 0.35 keV for ssb and 8 keV for dsb[10]). The ratio of the action cross-sections for the ssb to those of the dsb ranging from 17 to 18 were about two thirds of the values in the 2.1 keV region. Our data may be compared with those of dry pBR322 plasmid DNA irradiated with γ-rays under vacuum conditions[21]. The present values were one third of values in the literature; 180 eV for ssb and 3.2 keV for dsb (the unit has been converted to the unit of eV per strand break to make a direct comparison with our data), though the ssb/dsb ratio of 18 was in good agreement with the present values. Comparisons between the data for independent photon sources should be made carefully because of deferent irradiation conditions such as DNA concentration, the presence of additives, and different methods of dosimetry. Although further studies are no doubt needed in respect of these experimental conditions, it would be plausible to assume that the ultrasoft X-ray photons under 1 keV are more efficient than the higher energy photons, 2.1 keV and γ-ray photons.

The initial energy spectrum of the secondary electrons

The secondary electron equilibrium was considered to hold in the dried sample because the sample thickness (0.35 g/m^2, see MATERIALS AND METHODS) was fourteen times larger than the maximum range (2.5×10^{-2} g/m^2) of the secondary electrons with the highest energy (0.52 keV)[20] and than the continuous-slowing-down approximation range (2.52×10^{-2} g/m^2) of 0.5 keV electrons in solid dry DNA[22]. This fact proves the absorbed dose concept is applicable to

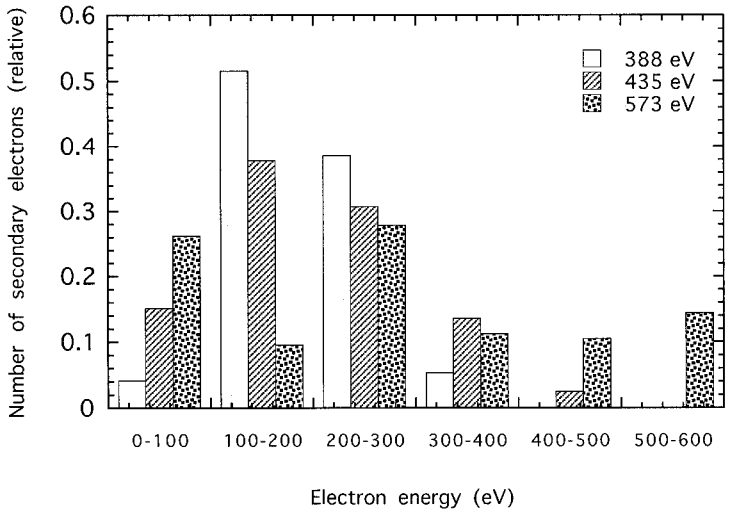

Fig. 6. Calculated energy spectrum of the Auger- and photo electrons generated with photoabsorption by the elements in the sample.

our experiments.

The initial energy spectrum of the secondary electrons in the sample at the three photon energies was calculated using the mass photoabsorption cross-sections in Table 5. The energies of the Auger electrons and the branching ratio of each Auger transition were used in the tables by Coghlan et al[23]. The fluorescent yields of each element were taken into account using the theoretical data[24]. The calculated spectra in 100 eV intervals are shown in Fig. 6, and indicate that the secondary electrons predominantly distributed from 100 to 400 eV at the photon energy of 388 and 435 eV, but at 573 eV, the electrons above 400 eV mainly originated from the KLL Auger electrons of the oxygen atom. Our experimental data showed that the difference of energy spectra of the secondary electrons among the photon energies would not affect the number of strand breaks per absorbed dose.

ACKNOWLEDGEMENTS

We gratefully acknowledge Mr. Yoshiro Kishi (Rikkyo University) for his valuable help with the Nomarski interference optics operation. This work was performed under the approval of the Photon Factory Advisory Committee (proposal No. 94G299).

REFERENCES

1. Goodhead, D.T., Munson, R.J., Thacker, J. and Cox, R. (1980) Mutation and inactivation of cultured mammalian cells exposed to beams of accelerated heavy ions. IV. Biophysical interpretation. Int. J. Radiat. Biol. **37**: 135–167.

2. Goodhead, D.T, Charlton, D.E., Wilson, W.E. and Paretzke, H.G. (1985) Current biophysical approaches to the understanding of biological effects of radiation in terms of local energy deposition. In: Proceedings of the Fifth Symposium on Neutron Dosimetry, Eds. H. Schraube, M. Burger and J. Booz (Luxembourg, Commission of the European Communities), EUR 9762 En, pp. 57–68.
3. Ward, J.F. (1988) DNA damage produced by ionizing radiation in mammalian cells: identities, mechanisms of formation and reparability. Prog. Nucleic Acid Res. Mol. Biol. **35**: 95–125.
4. Kobayashi, K., Hieda, K., Maezawa, Ando, M. and Ito, T. (1987) Monochromatic X-ray irradiation system (0.08–0.4 nm) for radiation biology studies using synchrotron radiation at the Photon Factory. J. Radiat. Res. **28**: 243–253.
5. Kobayashi, K., Hieda, K., Maezawa, H., Furusawa, Y., Suzuki, M. and Ito, T. (1991) Effects of K-shell X-ray absorption of intracellular phosphorus on yeast cells. Int. J. Radiat. Biol. **59**: 643–650.
6. Hieda, K. and Ito, T. (1991) Radiobiological experiments in the X-ray region with synchrotron radiation. In: Handbook on Synchrotron Radiation, Vol. 4. Eds. S. Ebashi, M. Koch and E. Rubenstein, pp. 431–465, Elsevier Science Publisher, North-Holland, Amsterdam.
7. Ito, T., Saito, M. and Kobayashi, K. (1992) Dissociation of a model DNA compound dApdA by monochromatic soft X-rays in0solids and comments on the high selectivity for 3' breakage in the phosphodiester bond. Int. J. Radiat. Biol. **62**: 129–136.
8. Yamada, H., Kobayashi, K. and Hieda, K. (1993) Effects of the K-shell X-ray absorption of phosphorus on the scission of the pentadeoxythimidylic acid. Int. J. Radiat. Biol. **63**: 151–159.
9. Takakura, K., Maezawa, H., Kobayashi, K. and Hieda, K. (1994) Strand Breaks in DNA in Buffered Solution Induced by Monochromatic X-tray around the K-shell Absorption Edge of Phosphorus. In: Synchrotron Radiation in the Biosciences, Eds. B. Chance, J. Deisenhofer, S. Ebashi, D.T. Goodhead, J.R. Helliwell, H.E. Huxley, T. Iizuka, J. Kirz, T. Mitsui, E. Rubenstein, N. Sakabe, T. Sasaki, G. Schmahl, H.B. Stuhrmann, K. W¸thrich and G. Zaccai, pp. 754–764, Oxford University Press, Oxford.
10. Hieda, K., Hirono, T., Azami, A., Suzuki, M., Furusawa, Y., Maezawa, H., Usami, N., Yokoya, A. and Kobayashi, K. (1996) Single- and double-strand breaks in pBR322 plasmid DNA by monochromatic X-rays on and off the K-absorption peak of phosphorus. Int. J. Radiat. Biol. **70**: 437–445.
11. Ade, H., Zhang, X., Cameron, S., Costello, C., Kirz, J. and Williams, S. (1992) Chemical contrast in x-ray microscopy and spatially resolved XANES spectroscopy of organic specimens. Science **258**: 972–975.
12. Kirtley, S.M., Mullins, O.C., Chen, J., van Elp, J., George, S.J, Chen, C.T., O'Halloran, T. and Cramer, S.P. (1992) Nitrogen chemical structure in DNA and related molecules by X-ray absorption spectroscopy. Biochim. Biophys. Acta **1132**: 249–254.
13. Falk, M., Hartman Jr, K.A. and Lord, R.C. (1963) Hydration of Deoxyribonucleic acid. III. A spectroscopic study of the effect of hydration on the structure of deoxyribonucleic acid. J. Am. Chem. Soc. **85**: 391–394.
14. Sambrook, J.E., Frisch, F. and Maniatis, T. (1989) Molecular Cloning, Cold Spring Harbor Laboratory Press, New York.
15. Tao, N.J., Lindsay, S.M. and Rupprecht, A (1989) Structure of DNA hydration shells studied by Raman spectroscopy. Biopolymers **28**: 1019–1030.
16. Hitchcock, A.P. and Brion, C.E. (1980) K-shell excitation spectra of CO, N2, and O2. J. Electron Spectroscopy and Related Phenomena **18**: 1–21.
17. Henke, B.L., Gullikson, E.M. and Davis, J.C. (1993) X-ray interactions: photoabsorption, scattering, transmission, and reflection at E = 50–30,000 eV, Z = 1–92. Atomic Data and Nuclear Data Tables **54**: 181–342.
18. Povirk, L.F., W¸bker, W. and Khnlein, W. (1977) DNA double-strand breaks and alkali-labile bonds produced by bleomycin. Nucleic Acid Res. **4**: 3573–3580.
19. Kornberg, A. (1960) Biological synthesis of deoxyribonucleic acid. Science **131**: 1503–1508.
20. International Commission on Radiation Units and Measurements. (1970) Linear Energy Transfer, ICRU Report 16, p. 27, International Commission on Radiation Units and Measurements, Washington D.C.
21. Ito, T., Baker, S.C., Stickley, C.D., Peak, J.G. and Peak, M.J. (1993) Dependence of the yield of strand breaks induced by γ -rays in DNA on the physical conditions of exposure: water content and temperature. Int. J. Radiat. Biol. **63**: 289–296.

22. LaVerne, J.A. and Pimblott, S.M. (1995) Electron energy-loss distribution in solid, dry DNA. Radiat. Res. **141**: 208–215.
23. Coghlan, W.A. and Clausing, R.E. (1973) Auger catalog calculated transition energies listed by energy and element. Atomic Data **5**: 317–469.
24. Rambynek, W., Crasemann, B., Fink, R.W., Freund, H.U., Mark, H., Swift, C.D. and Price, R.E. (1972) X-ray Fluorescence Yields, Auger, and Coster-Kronig Transition Probabilities. Rev. Modern Phys. **44**: 716–813.